

Quantum features of a non-commutative Schwarzschild black hole

A. A. Araújo Filho,^{1,2,3,*} I. P. Lobo,^{4,2,†} P. H. M. Barros,^{5,6,‡} and Amilcar R. Queiroz^{2,§}

¹*Departamento de Física, Universidade Federal da Paraíba,
Caixa Postal 5008, 58051-970, João Pessoa, Paraíba, Brazil.*

²*Departamento de Física, Universidade Federal de Campina Grande Caixa Postal 10071,
58429-900 Campina Grande, Paraíba, Brazil.*

³*Center for Theoretical Physics, Khazar University,
41 Mehseti Street, Baku, AZ-1096, Azerbaijan.*

⁴*Department of Chemistry and Physics, Federal University of Paraíba,
Rodovia BR 079 - km 12, 58397-000 Areia-PB, Brazil*

⁵*Departamento de Física, Universidade Federal do Piauí (UFPI),
Campus Min. Petrônio Portella, Teresina - PI, 64049-550, Brazil*

⁶*Departamento de Matemática e Física,
Universidade Estadual do Maranhão (UEMA), Caxias - MA, 65604-380, Brazil*

(Dated: January 21, 2026)

Abstract

This work aims to present the quantum aspects of a non-commutative gauge gravity formulation of a Schwarzschild-like black hole constructed via the Moyal twist $\partial_t \wedge \partial_\theta$. Particle creation is estimated for bosonic and fermionic fields using the quantum tunneling method, with divergent integrals treated through the residue prescription. Since the surface gravity is well defined for this configuration, the corresponding emission rates and evaporation lifetimes are also computed. In addition, previously reported results in the literature on gauge gravity Schwarzschild black holes are revisited. Finally, we infer constraints on the non-commutative parameter Θ from solar-system tests.

^{*}Electronic address: dilto@fisica.ufc.br

[†]Electronic address: lobofisica@gmail.com

[‡]Electronic address: phmbarros@ufpi.edu.br

[§]Electronic address: amilcarq@df.ufcg.edu.br

Contents

I. Introduction	2
II. The modified Schwarzschild black hole	4
III. Quantum aspects	5
A. Particle creation for bosons	5
B. Particle production for fermions	7
IV. Black hole evaporation and radiative emission	10
V. Bounds	13
A. Perihelion precession of Mercury	13
B. Deflection of light	14
C. Time delay of light	14
VI. Conclusion	15
Acknowledgments	16
Data Availability Statement	17
References	17

I. INTRODUCTION

Classical general relativity places no built-in bound on the precision with which distances can be resolved. By contrast, a wide class of quantum-gravity–motivated approaches point toward the emergence of a smallest measurable length, typically tied to the Planck scale. This expectation has led to the formulation of spacetime models in which the coordinates fail to commute, providing an effective way to encode such a cutoff at short distances [1–3]. Frameworks of this type have also become standard tools in the study of supersymmetric gauge field theories, where their structural and renormalization properties have been examined in detail [4]. When gravitational backgrounds are considered, non-commutative corrections are commonly implemented through the Seiberg–Witten map, which deforms the underlying symmetry content of the geometry while preserving gauge consistency [5].

Over the past years, non-commutative constructions have been widely employed as an alternative route to explore black hole physics beyond the classical geometric picture [6–15]. Within this line of investigation, particular attention has been devoted to understanding how departures from

ordinary spacetime commutativity reshape the dynamical evolution of black holes, with emphasis on the mechanisms governing particle emission and mass loss [16, 17]. Alongside these dynamical aspects, the introduction of non-commutative corrections has been shown to modify the thermodynamic description of black holes, motivating systematic analyses of quantities such as entropy, Hawking temperature, and heat capacity in a variety of scenarios [14, 18–21].

A departure from classical spacetime geometry can be implemented by promoting the coordinates to non-commuting operators that satisfy the algebra $[x^\mu, x^\nu] = i\Theta^{\mu\nu}$, where the antisymmetric tensor $\Theta^{\mu\nu}$ encodes the scale and structure of the deformation. This modification replaces the conventional notion of a smooth manifold with an effective description in which short-distance behavior is intrinsically altered. Several formalisms have been proposed to accommodate such a deformation within gravitational theories. One particularly systematic construction is based on deforming the gauge symmetry underlying gravity: starting from a de Sitter-type group $SO(4,1)$, the theory is consistently mapped onto the Poincaré group $ISO(3,1)$ through the Seiberg–Witten prescription. Within this gauge-theoretic setting, Chaichian and collaborators [22] obtained a Schwarzschild-like solution whose metric explicitly reflects non-commutative corrections.

Recent developments have reconsidered how black hole geometries are obtained in non-commutative gauge theory. In particular, the analysis carried out in Ref. [23] reformulated the construction procedure and demonstrated that the method originally proposed in Ref. [22] was incomplete. The reassessment showed that the earlier formulation omitted a necessary contribution in the non-commutative sector through the following term:

$$-\frac{1}{16}\Theta^{\nu\rho}\Theta^{\lambda\tau}\left[\tilde{\omega}_\nu^{ac}\tilde{\omega}_\lambda^{cd}\left(D_\tau R_{\rho\mu}^{d5} + \partial_\tau R_{\rho\mu}^{d5}\right)\right].$$

This omission propagated into the tetrad sector, producing nontrivial modifications of the vierbein fields and, as a direct consequence, altering the associated metric components.

Over the last year, a number of studies have addressed thermodynamics and particle creation in the framework of non-commutative gauge theory [24–27]. More recent analyses, however, have revisited the underlying construction and revealed the presence of inconsistencies in part of the existing literature [23]. Along these lines, Refs. [28, 29] advanced the discussion by explicitly identifying and clarifying some of these shortcomings. Even so, the corrections proposed so far remain limited to specific Moyal twists, namely $\partial_r \wedge \partial_\theta$ and $\partial_t \wedge \partial_r$, for which the surface gravity is not well defined. As a result, some important quantities such as the thermodynamic functions, the evaporation lifetime, and the emission rate cannot be consistently determined in those configurations.

In order to resolve this limitation and address the open gap in the literature, the present work investigates quantum effects—specifically particle creation, evaporation, and emission rate—for a Schwarzschild-like black hole in non-commutative gauge theory constructed with the Moyal twist $\partial_t \wedge \partial_\theta$. For this choice, in agreement with Ref. [23], the surface gravity is well defined, which allows

all these aspects to be treated consistently. In addition, to reinforce the physical robustness of the analysis, bounds on the non-commutative parameter Θ are obtained from solar-system tests.

II. THE MODIFIED SCHWARZSCHILD BLACK HOLE

As it was pointed out above, Ref. [23] revisited and corrected the procedure previously proposed in Ref. [22] for constructing black hole solutions within non-commutative gauge theory. As a consequence of this revision, all geometries obtained through that prescription are modified, as explicitly illustrated by the comparison performed for the Hayward spacetime [30]. In particular, Ref. [23] shows that, for diagonal metrics, three distinct Schwarzschild-like solutions emerge depending on the choice of Moyal twist, namely $\partial_r \wedge \partial_\theta$, $\partial_t \wedge \partial_r$, and $\partial_t \wedge \partial_\theta$. Among these possibilities, only the $\partial_t \wedge \partial_\theta$ deformation leads to a well-defined surface gravity. Since the present analysis focuses on particle creation and evaporation, we adopt precisely this configuration to ensure the consistency of the thermodynamic quantities. The corresponding solution associated with the (t, θ) Moyal twist is therefore presented below [23]:

$$\begin{aligned} g_{tt}(r, \Theta) &= -\left(1 - \frac{2M}{r}\right) + \frac{M^2(-2M + r)(-30M + 9r)}{48r^6}\Theta^2, \\ g_{rr}(r, \Theta) &= \left(1 - \frac{2M}{r}\right)^{-1} - \frac{M(11M^2 - 10Mr + 2r^2)}{4r^4(-2M + r)}\Theta^2, \\ g_{\theta\theta}(r, \Theta) &= r^2 + \frac{M(11M - 4r)(2M - r)}{16r^3}\Theta^2, \\ g_{\varphi\varphi}(r, \Theta) &= r^2 \sin^2 \theta + \frac{M(-2M + r)(M + r) \sin^2 \theta}{4r^3}\Theta^2. \end{aligned} \quad (1)$$

The presence of the Moyal deformation $\partial_t \wedge \partial_\theta$ explicitly breaks the original spherical symmetry of the geometry. As a consequence, the resulting spacetime departs from the standard isotropic structure. The modified line element contains two distinguished radial loci: the origin at $r = 0$, where the curvature diverges and a genuine singularity occurs, and the hypersurface $r = 2M$, which continues to represent the event horizon and simultaneously defines a Killing horizon. Notably, the non-commutative modification does not shift the horizon radius, which remains fixed at its “classical value”. In addition, the corresponding surface gravity associated with this horizon is then expressed as [23]

$$\kappa^2 = \frac{M^2}{r^4} + \frac{(154M^5 - 117M^4r + 20M^3r^2)}{16r^9}\Theta^2 + \mathcal{O}(\Theta^3). \quad (2)$$

Evaluating the geometry at $r = 2M$ shows that the contribution proportional to Θ^2 drops out identically, yielding a surface gravity $\kappa = 1/(4M)$. This result demonstrates that the non-commutative parameter does not modify the surface gravity as well. Consequently, because both the horizon position and κ remain unchanged under the Θ deformation, the thermodynamic quantities coincide

with those of the standard Schwarzschild black hole. However, the particle creation process—both for bosonic and fermionic fields—as well as the evaporation lifetime and the emission rate, are affected by the non-commutative parameter Θ . The subsequent section is devoted to the investigation of these effects.

III. QUANTUM ASPECTS

A. Particle creation for bosons

To incorporate backreaction effects associated with energy balance in the emission process, we adopt a semiclassical strategy inspired by earlier tunneling analyses [31–34]. The starting point consists in performing a coordinate transformation that casts the geometry into a Painlevé–Gullstrand–type representation, which is regular across the horizon [33, 34]. In this framework, the line element assumes the form $ds^2 = -f(r, \Theta) dt^2 + 2h(r, \Theta) dt dr + dr^2 + z(r, \theta, \Theta) d\theta^2 + y(r, \theta, \Theta) d\varphi^2$, where the mixed component $h(r, \Theta)$ is fixed by the requirement that the spatial slices remain flat, yielding [34] $h(r, \Theta) = \sqrt{f(r, \Theta)(g(r, \Theta)^{-1} - 1)}$.

Once the metric is expressed in this form, the quantum emission process follows from the nontrivial contribution to the imaginary sector of the particle’s action [32, 33]. The tunneling amplitude is therefore controlled by the classical action evaluated along a forbidden trajectory. For a massless excitation, this action is written as $S = \int p_\mu dx^\mu$.

In evaluating the imaginary part of the action, the temporal sector does not generate any complex contribution. Indeed, the term $p_t dt = -\omega dt$ remains strictly real along the trajectory and therefore plays no role in the emergence of an imaginary component. As a consequence, the complex part of the action originates solely from the integration along the radial direction, which provides the only nontrivial contribution to $\text{Im } S$

$$\text{Im } S = \text{Im} \int_{r_i}^{r_f} p_r dr = \text{Im} \int_{r_i}^{r_f} \int_0^{p_r} dp'_r dr. \quad (3)$$

To incorporate the energy carried away during the quantum emission, the Hamiltonian is parametrized as $H = M - \omega'$, with ω' denoting the running energy of the escaping particle. Under this parametrization, Hamilton’s equation directly implies $dH = -d\omega'$. Allowing ω' to interpolate between 0 and the final value ω , which corresponds to the total radiated energy. In this manner, the associated term entering the imaginary sector of the action can then be written in the following form:

$$\text{Im } S = \text{Im} \int_{r_i}^{r_f} \int_M^{M-\omega} \frac{dH}{dr/dt} dr = \text{Im} \int_{r_i}^{r_f} dr \int_0^\omega -\frac{d\omega'}{dr/dt}. \quad (4)$$

By interchanging the sequence of integrations and performing a suitable change of variables, the

original integral can be recast into the form:

$$\begin{aligned}\frac{dr}{dt} &= -h(r, \Theta) + \sqrt{f(r, \Theta) + h(r, \Theta)^2} \\ &= -\frac{\sqrt{-M(\Theta^2 M^2(10M - 3r) + 16r^5)(11\Theta^2 M^2 + 2\Theta^2 r(r - 5M) - 4r^4)}}{4\sqrt{2}r^5} \\ &\quad + \frac{\sqrt{(\Theta^2 M^2(10M - 3r) + 16r^5)(\Theta^2 M(-11M^2 + 10Mr - 2r^2) + 2r^5)}}{4\sqrt{2}r^5}.\end{aligned}\quad (5)$$

Here, the backreaction induced by the emitted quantum is incorporated by promoting the mass parameter to a dynamical quantity. This is achieved through the shift $M \rightarrow (M - \omega')$, which alters the background geometry accordingly and results in an updated form of the metric function, written as:

$$\text{Im } S \approx \text{Im} \int_0^\omega -d\omega' \times \int_{r_i}^{r_f} \frac{dr}{\left(1 - \sqrt{2}\sqrt{\frac{M - \omega'}{r}}\right) + \Theta^2 \Xi(r, M, \Theta)}, \quad (6)$$

where Ξ is given by

$$\begin{aligned}\Xi(r, M, \Theta) &= \frac{1}{4\sqrt{2}r^5} \times \left[-\frac{16r^2(M - \omega') - 77r(M - \omega')^2 + 78(M - \omega')^3}{4\sqrt{2}} \right. \\ &\quad \left. - \frac{1}{4}\sqrt{\frac{M - \omega'}{r}}(40r^2(M - \omega') - 47r(M - \omega')^2 + 10(M - \omega')^3 - 8r^3) \right].\end{aligned}\quad (7)$$

For clarity, introduce the shorthand $\Delta(r, \omega') \equiv 2(M - \omega')$. Under the replacement $M \rightarrow (M - \omega')$, the singular structure of the integrand is displaced, so that the pole is no longer located at the original horizon but instead occurs at the shifted radius $r = 2(M - \omega')$. Evaluating the integral by deforming the contour to encircle this pole in the counterclockwise sense then yields:

$$\text{Im } S = 2\pi\omega(2M - \omega) + \frac{1}{64}\pi\Theta^2 \left[\ln(M) - \ln(M - \omega) \right]. \quad (8)$$

Following this procedure, the probability for the emission of a *Hawking* quantum—now incorporating the non-commutative modifications—can be written in the form:

$$\Gamma(\omega, \Theta) \sim e^{-2\text{Im } S} = e^{-4\pi\omega(2M - \omega) - \frac{1}{32}\pi\Theta^2 \left[\ln(M) - \ln(M - \omega) \right]}. \quad (9)$$

Moreover, the occupation number (particle number density) can be written directly in terms of the tunneling probability as follows:

$$n(\omega, \Theta) = \frac{\Gamma(\omega, \Theta)}{1 - \Gamma(\omega, \Theta)} = \frac{1}{\exp \left\{ \frac{1}{32}\pi\Theta^2 [\ln M - \ln(M - \omega)] + 4\pi\omega(2M - \omega) \right\} - 1}. \quad (10)$$

To display the behavior of $n(\omega, \Theta)$, Fig. 1 is presented. We observe that, for increasing values of Θ , the associated particle number density decreases as the frequency ω increases.

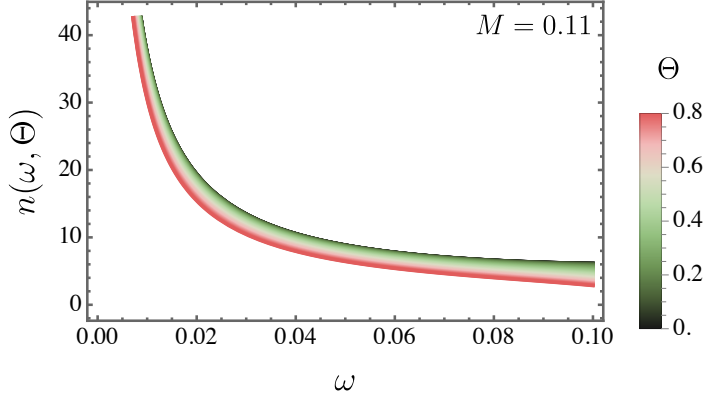


Figure 1: Bosonic particle production, quantified by $n(\omega, \Theta)$, is plotted as a function of the energy ω for different choices of the non-commutative parameter.

B. Particle production for fermions

The semiclassical description of fermion emission from a black hole horizon is developed by treating the spinor field as a probe propagating on a fixed curved background. Instead of introducing horizon-regular coordinates at the outset—an approach commonly adopted in earlier tunneling analyses based on Painlevé–Gullstrand or Kruskal–Szekeres constructions—the formulation here relies directly on the covariant field equations in the original coordinate system [35].

The behavior of a massive spin- $\frac{1}{2}$ field in this geometry follows from the curved-spacetime Dirac equation, $(\bar{\gamma}^\mu \bar{\nabla}_\mu + m) \bar{\Psi}_{\uparrow\downarrow}^\pm(x, \Theta) = 0$, where the non-commutative parameter Θ enters implicitly through the metric functions. The spinor covariant derivative is defined as $\bar{\nabla}_\mu = \partial_\mu + \frac{i}{2} \Gamma^\alpha_\mu \gamma^\beta, \bar{\Sigma}_{\alpha\beta}$, with the Lorentz generators given by $\bar{\Sigma}_{\alpha\beta} = \frac{i}{4}, [\bar{\gamma}_\alpha, \bar{\gamma}_\beta]$.

The spacetime coordinates are chosen as $x = (t, r, \theta, \varphi)$. The matrices $\bar{\gamma}^\mu$ provide a curved-space representation of the Clifford algebra and satisfy the anticommutation relation $\{\bar{\gamma}_\alpha, \bar{\gamma}_\beta\} = 2 g_{\alpha\beta} \mathbb{1}$, where $\mathbb{1}$ denotes the 4×4 identity matrix. For later convenience, the metric coefficients are rewritten in the form $g_{tt}(r, \Theta) \equiv -A(r, \Theta)$, $g_{rr}(r, \Theta) \equiv B(r, \Theta)$, $g_{\theta\theta}(r, \Theta) \equiv C(r, \Theta)$, and $g_{\varphi\varphi}(r, \Theta) \equiv D(r, \Theta)$.

This parametrization isolates the radial structure responsible for horizon effects and prepares the ground for the semiclassical evaluation of fermionic tunneling probabilities. A suitable explicit representation of the $\bar{\gamma}$ matrices is then introduced to carry out the calculation

$$\begin{aligned} \bar{\gamma}^t(r, \Theta) &= \frac{i}{\sqrt{A(r, \Theta)}} \begin{pmatrix} 1 & \mathbf{0} \\ \mathbf{0} & -1 \end{pmatrix}, \quad \bar{\gamma}^r(r, \Theta) = \sqrt{\frac{1}{B(r, \Theta)}} \begin{pmatrix} \mathbf{0} & \sigma_3 \\ \sigma_3 & \mathbf{0} \end{pmatrix}, \\ \bar{\gamma}^\theta(r, \Theta) &= \frac{1}{\sqrt{C(r, \Theta)}} \begin{pmatrix} \mathbf{0} & \sigma_1 \\ \sigma_1 & \mathbf{0} \end{pmatrix}, \quad \bar{\gamma}^\varphi(r, \Theta) = \frac{1}{\sqrt{D(r, \Theta)}} \begin{pmatrix} \mathbf{0} & \sigma_2 \\ \sigma_2 & \mathbf{0} \end{pmatrix}. \end{aligned}$$

In the present formulation, the matrices σ are introduced as the generators of the two-dimensional spinor sector. Their multiplication law follows directly from their defining properties and can be compactly expressed as $\sigma_i \sigma_j = \delta_{ij} \mathbb{1} + i \varepsilon_{ijk} \sigma_k$, with the indices i, j, k running over 1, 2, 3. Beyond

this algebraic structure, the chirality operator acquires a modified form due to the influence of non-commutativity. In this context, the matrix $\gamma^5(r, \Theta)$ is no longer treated as a purely constant object but instead reflects the underlying geometric deformation. Its explicit realization is therefore identified with the following matrix structure:

$$\gamma^5(r, \Theta) = i\gamma^t(r, \Theta)\gamma^r(r, \Theta)\gamma^\theta(r, \Theta)\gamma^\varphi(r, \Theta) = i\sqrt{\frac{1}{A(r, \Theta)B(r, \Theta)C(r, \Theta)D(r, \Theta)}} \begin{pmatrix} \mathbf{0} & -\mathbf{1} \\ \mathbf{1} & \mathbf{0} \end{pmatrix}.$$

A fermionic configuration with spin aligned along the outward radial direction is described by adopting the following spinor ansatz [32]:

$$\psi_\uparrow^{(+)}(x, \Theta) = \begin{pmatrix} H_\uparrow^{(+)}(x, \Theta) \\ 0 \\ Y_\uparrow^{(+)}(x, \Theta) \\ 0 \end{pmatrix} \exp\left[i\psi_\uparrow^{(+)}(x, \Theta)\right]. \quad (11)$$

The discussion is restricted to the sector in which the fermionic spin is aligned with the outward radial direction, labeled by the (+) polarization. The opposite orientation, denoted by (-), follows from the same reasoning and therefore is not treated separately. Upon substituting the corresponding spinor ansatz, given in Eq. (11), into the curved-space Dirac equation, a coupled system of relations emerges. This step follows the semiclassical tunneling prescription developed in Ref. [32], although the present formulation is adapted to the geometry under consideration.

In carrying out the calculation, only the dominant terms in the \hbar expansion are kept, while higher-order quantum corrections are discarded. To separate the dynamical variables, the classical action is assumed to take the form $\psi_\uparrow^{(+)} = -\omega t + \chi(r, \Theta) + L(\theta, \varphi)$, which allows the temporal, radial, and angular contributions to be treated independently, leading to the relations discussed below [32]

$$+ \frac{i\omega H_\uparrow^{(+)}(x, \Theta)}{\sqrt{A(r, \Theta)}} - \sqrt{\frac{1}{B(r, \Theta)}} Y_\uparrow^{(+)}(x, \Theta) \chi'(r, \Theta) + m H_\uparrow^{(+)}(x, \Theta) = 0, \quad (12)$$

$$- Y_\uparrow^{(+)}(x, \Theta) \left(\frac{\partial_\theta L(\theta, \varphi)}{\sqrt{C(r, \Theta)}} + \frac{i\partial_\varphi L(\theta, \varphi)}{\sqrt{D(r, \Theta)}} \right) = 0, \quad (13)$$

$$- \frac{i\omega Y_\uparrow^{(+)}(x, \Theta)}{\sqrt{A(r, \Theta)}} - \sqrt{\frac{1}{B(r, \Theta)}} H_\uparrow^{(+)}(x, \Theta) \chi'(r, \Theta) + m Y_\uparrow^{(+)}(x, \Theta) = 0, \quad (14)$$

$$- H_\uparrow^{(+)}(x, \Theta) \left(\frac{\partial_\theta L(\theta, \varphi)}{\sqrt{C(r, \Theta)}} + \frac{i\partial_\varphi L(\theta, \varphi)}{\sqrt{D(r, \Theta)}} \right) = 0. \quad (15)$$

The explicit functional forms of $H_\uparrow^{(+)}(x, \Theta)$ and $Y_\uparrow^{(+)}(x, \Theta)$ do not play a decisive role in what follows. What matters instead is that the simultaneous validity of Eqs. (13) and (15) imposes a

nontrivial restriction on the angular sector, namely $\frac{\partial_\theta L(\theta, \varphi)}{\sqrt{C(r, \Theta)}} + \frac{\text{i} \partial_\varphi L(\theta, \varphi)}{\sqrt{D(r, \Theta)}} = 0$. This condition forces the angular contribution $L(\theta, \varphi)$ to be complex. The same requirement arises for both emission and absorption channels, implying that the angular dependence contributes identically to ingoing and outgoing solutions. Consequently, such terms drop out when forming the ratio of tunneling probabilities, and they can be omitted from the remainder of the computation. This cancellation mechanism is consistent with earlier semiclassical analyses of fermionic tunneling [32].

Specializing now to the massless limit, $m = 0$, the remaining radial equations decouple and admit two independent branches. These solutions are characterized by the relations $H_\uparrow^{(+)}(x, \Theta) = -\text{i} Y_\uparrow^{(+)}(x, \Theta)$, $\chi'(r, \Theta) = \chi'_{\text{out}}(r, \Theta) = \frac{\omega}{\sqrt{A(r, \Theta)/B(r, \Theta)}}$, and $H_\uparrow^{(+)}(x, \Theta) = \text{i} Y_\uparrow^{(+)}(x, \Theta)$, $\chi'(r, \Theta) = \chi'_{\text{in}}(r, \Theta) = -\frac{\omega}{\sqrt{A(r, \Theta)/B(r, \Theta)}}$. The two branches are naturally interpreted as describing outward-moving and inward-moving modes, respectively, through the horizon [32].

Within this semiclassical picture, the tunneling probability associated with fermionic emission is determined by the imaginary part of the radial action. It can be written as $\Gamma_\psi(\Theta, \omega) \sim \exp[-2 \text{Im}(\chi_{\text{out}}(r, \Theta) - \chi_{\text{in}}(r, \Theta))]$. Using the symmetry between the two branches, the radial actions satisfy $\chi_{\text{out}}(r, \Theta) = -\chi_{\text{in}}(r, \Theta) = \int dr \frac{\omega}{\sqrt{A(r, \Theta)/B(r, \Theta)}}$, which completes the derivation of the tunneling rate in the present setup.

A subtle but relevant assumption enters at this stage of the analysis. The deformation parameter Θ is treated as a small quantity, a hypothesis that will later be corroborated by bounds obtained from solar system tests. Under this premise, the metric functions vary smoothly near the horizon and can be approximated by their first-order expansions around $r = r_h$.

This local linear behavior implies that the horizon contribution to the radial action is governed by a simple singular structure. As a result, the integrals that determine the imaginary part of the action acquire a first-order pole at $r = r_h$. Such a feature permits a straightforward evaluation using standard complex analysis prescriptions, leading directly to the expression written below

$$A(r, \Theta) \frac{1}{B(r, \Theta)} \approx A(r, \Theta) \left(\frac{1}{B(r, \Theta)} \right)' (r - r_h)^2 + \dots \quad (16)$$

By implementing Feynman's prescription to regulate the pole at the horizon, the radial integral can be evaluated explicitly, leading to the result stated below:

$$2\text{Im} [\chi_{\text{out}}(r, \Theta) - \chi_{\text{in}}(r, \Theta)] = \text{Im} \int dr \frac{4\omega}{\sqrt{\frac{A(r, \Theta)}{B(r, \Theta)}}} = \frac{2\pi\omega}{\kappa(r, \Theta)}, \quad (17)$$

with κ being given by

$$\kappa(r, \Theta) \Big|_{r=r_h} \approx \frac{M}{r_h^2} + \frac{M(294M^3 - 330M^2r_h + 115Mr_h^2 - 12r_h^3)}{16r_h^7} \Theta^2 = \frac{1}{4M} - \frac{\Theta^2}{1024M^3}. \quad (18)$$

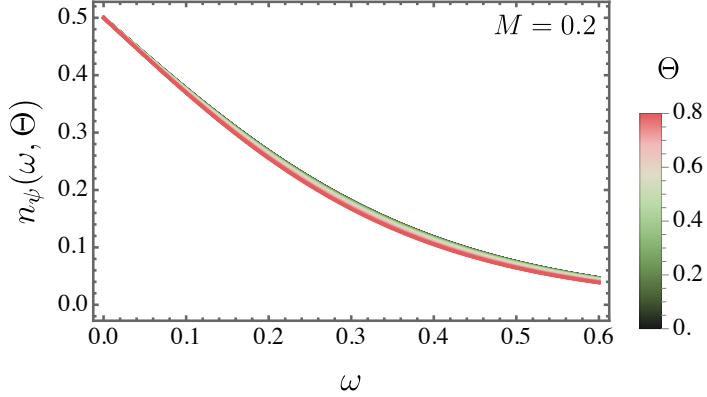


Figure 2: Fermionic particle production spectra $n_\psi(\omega, \Theta)$ plotted versus the frequency ω for different choices of the non-commutative parameter Θ .

For fermionic modes propagating on the black hole background, the tunneling rate fixes the occupation factor of the emitted particles. This rate takes the Boltzmann-type form $\Gamma_\psi(\omega, \Theta) \sim \exp\left(-\frac{2\pi\omega}{\kappa(r, \Theta)}\right)$. Replacing $\kappa(r, \Theta)$ by its value evaluated at the horizon position $r = r_h$ leads to the expression given below

$$n_\psi(\omega, \Theta) = \frac{\Gamma_\psi(\omega, \Theta)}{1 + \Gamma_\psi(\omega, \Theta)} = \frac{1}{\exp\left(\frac{2048\pi M^3 \omega}{256M^2 - \Theta^2}\right) + 1}. \quad (19)$$

Figure 2 displays the fermionic particle-creation density $n_\psi(\omega, \Theta)$. The plot shows a monotonic suppression of the production rate as Θ increases, indicating that larger non-commutative deformations reduce the emitted fermion flux.

IV. BLACK HOLE EVAPORATION AND RADIATIVE EMISSION

This section examines the evaporation process of the black hole at a qualitative level. The discussion relies on the use of the *Stefan–Boltzmann* relation as a practical tool to estimate the radiative energy loss associated with thermal emission, following the standard approach adopted in previous studies [36, 37]

$$\frac{dM}{dt} = -\alpha a \tilde{\sigma} T^4. \quad (20)$$

Here, $\tilde{\sigma}$ represents the effective radiating area, while a denotes the radiation constant and α encodes the greybody correction. The temperature T corresponds to the Hawking value, $T = 1/(8\pi M)$. The emitted flux is dominated by massless species—most notably photons and neutrinos—consistent with standard evaporation analyses [38, 39]. In the geometric-optics regime, the absorption cross section can be approximated by $\sigma \simeq \pi R_{\text{sh}}^2$, where R_{sh} is the shadow radius and plays the role of an effective emission scale. In this limit, often denoted $\tilde{\sigma}_{\text{lim}}$, the greybody factor approaches unity, $\alpha \rightarrow 1$, as discussed in [40]. After straightforward algebraic manipulation,

the limiting cross section σ_{lim} reads

$$\tilde{\sigma}_{\text{lim}} = \pi \left(\frac{5\Theta^2}{288\sqrt{3}M} + 3\sqrt{3}M \right)^2 \approx 27\pi M^2 + \frac{5\pi\Theta^2}{48}, \quad (21)$$

where terms of order higher than Θ^2 have been neglected in the above expression.

The existence of thermal emission from black holes was established in the seminal work of Ref. [41], where the radiation spectrum was shown to be characterized by a well-defined temperature. While equivalent derivations based on Bogoliubov coefficients are available in the literature, they are not pursued here. Within the framework developed above, the relation in Eq. (20) can therefore be rewritten as follows:

$$\frac{dM}{dt} = - \frac{\left(\frac{5\pi\Theta^2}{48} + 27\pi M^2 \right)}{4096\pi^4 M^4}, \quad (22)$$

The expression is truncated at second order in Θ , which allows a more compact form to be obtained. For convenience, the product of constants is fixed by choosing $a\alpha = 1$. With these choices in place, the analysis proceeds by computing the integral given below:

$$\int_0^{t_{\text{evap}}} d\tau = \int_{M_i}^{M_f} \left[-\frac{\left(\frac{5\pi\Theta^2}{48} + 27\pi M^2 \right)}{4096\pi^4 M^4} \right]^{-1} dM. \quad (23)$$

The quantity t_{evap} represents the complete lifetime of the black hole. Within the approximations adopted here, this timescale is expressed as:

$$t_{\text{evap}} \approx \frac{1280\pi^3\Theta^2(M_f - M_i)}{2187} - \frac{4096}{81} (\pi^3 (M_f^3 - M_i^3)), \quad (24)$$

where contributions beyond second order in Θ have also been discarded.

The evaporation timescale t_{evap} follows from a fully analytic computation. Since the spacetime considered here does not support the formation of a stable remnant, the evaporation process is taken to proceed until the mass vanishes. Accordingly, the final state is characterized by the limit $M_f \rightarrow 0$, which yields:

$$t_{\text{evap}} = \frac{4096\pi^3 M_i^3}{81\xi} - \frac{1280\pi^3\Theta^2 M_i}{2187}. \quad (25)$$

Figure 3 illustrates the evaporation behavior and shows that increasing the non-commutative parameter leads to a shorter black-hole lifetime. This trend is consistent with results reported for other non-commutative black hole models [42, 43]. The same tendency is confirmed below through the analysis of the corresponding emission rate.

Near the event horizon, quantum phenomena become dominant and allow vacuum fluctuations to generate short-lived particle pairs. In certain instances, one member of the pair acquires sufficient energy to penetrate the effective barrier and propagate to infinity through a tunneling process. The escape of this positive energy mode reduces the mass of the black hole and drives its

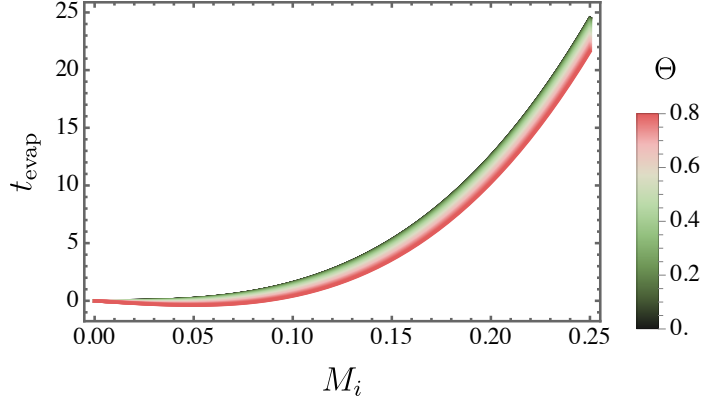


Figure 3: Total evaporation time t_{evap} as a function of the initial mass M_i for several values of the non-commutative parameter Θ .

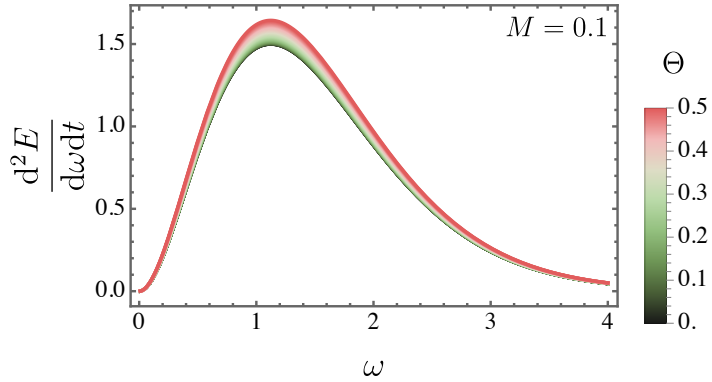


Figure 4: Emission rate as a function of the frequency ω for different values of the non-commutative parameter Θ .

evaporation, a mechanism identified with Hawking radiation. From the perspective of a distant observer, this mass loss is encoded in the high-energy absorption properties of the spacetime. In this limit, the absorption cross section approaches a constant value, conventionally denoted by $\tilde{\sigma}_{lim}$. As shown in Refs. [44, 45], this asymptotic behavior controls the form of the spectral energy flux, which can be written as follows:

$$\frac{d^2E}{d\omega dt} = \frac{2\pi^2\tilde{\sigma}_{lim}}{e^{\frac{\omega}{T}} - 1} \omega^3. \quad (26)$$

Here, ω labels the photon frequency. Substituting the corresponding parameters, the Hawking temperature into the emission formula yields the corrected expression for the radiated power:

$$\frac{d^2E}{d\omega dt} = \frac{\pi^3\omega^3(5\Theta^2 + 1296M^2)}{24(e^{8\pi M\omega} - 1)}. \quad (27)$$

Figure 4 shows that the emission rate grows as the non-commutative parameter Θ increases. This behavior is consistent with the reduction of the evaporation time discussed earlier.

V. BOUNDS

We can constrain the non-commutativity parameter by analyzing the classical tests of general relativity and estimating the magnitude of Θ that do not contradicts the experimental data. In order to do this, we consider the trajectory of Mercury as a test particle that follows a time-like geodesic and of light ray emitted by a distant source and bended by the Sun, and that reflected by the Cassini probe when grazing the surface of the Sun.

In the equatorial plane ($\theta = \pi/2$), the Lagrangian of test particles is given by

$$A(r)\dot{t}^2 - B^{(\Theta)}\dot{r}^2 - D^{(\Theta)}\dot{\varphi}^2 = \eta = -2\mathcal{L}, \quad (28)$$

where \mathcal{L} is the Lagrangian. When $\eta = 1$, we have time-like trajectories, and when $\eta = 0$ we have light-like trajectories. The conserved quantities, named energy E and angular momentum L are

$$E = A^{(\Theta)}\dot{t} \quad \text{and} \quad L = D^{(\Theta)}\dot{\varphi}. \quad (29)$$

By working with these conserved quantities, we can manipulate equation (28) to find a second order differential equation for the variable $u = L^2/(Mr)$ as

$$u''(\varphi) = \eta - u + 3\frac{M^2}{L^2}u^2 \left(1 + \frac{\Theta^2}{2L^2}(E^2 - \eta)\right). \quad (30)$$

We can see that the non-commutative parameter couples with the energy of the test particle, which is a property found in several quantum gravity scenarios that lead to interesting phenomenological opportunities [46, 47].

A. Perihelion precession of Mercury

From (30), we verify that if we fix $\eta = 1$, we are effectively redefining the mass of the central object that is responsible for the trajectory of the planet. This means that Mercury behaves as it is effectively surrounding a massive object of mass square

$$\widetilde{M}^2 = M^2 \left(1 + \frac{\Theta^2}{2L^2}(E^2 - \eta)\right). \quad (31)$$

To constrain the parameter Θ , we analyze the dimensionless perturbative term $\frac{\Theta^2}{2L^2}(E^2 - \eta)$. In a Keplerian orbit, the specific angular momentum L relates to the semi-major axis a and eccentricity e via $L^2 = Ma(1 - e^2)$, and the specific orbital energy per unit mass is $E = -M/(2a)$ [48].

Adopting natural units, we assign the Sun's mass as $M_\odot = 9.138 \times 10^{37}$. For Mercury, we use $a = 3.583 \times 10^{45}$ and $e = 0.2056$. From these, we compute $L = 5.600 \times 10^{41}$, which justifies

a perturbative treatment because M^2/L^2 is negligibly small. We also find $E^2 = 1.627 \times 10^{-16}$, confirming that corrections depending on energy are insignificant.

The general relativistic prediction for Mercury's perihelion advance is $\Delta\Phi_{\text{GR}} = 42.9814''$ per century. The observed value, $\Delta\Phi_{\text{Exp}} = (42.9794 \pm 0.0030)''$ per century [49, 50], agrees exceptionally well. By comparing the experimental uncertainty with our theoretical expression, we derive the allowed range (both signs of Θ^2 are kept in the analysis for completeness)

$$-3.725 \times 10^9 \text{ m}^2 \leq \Theta^2 \leq 1.862 \times 10^{10} \text{ m}^2.$$

B. Deflection of light

For the deflection of light, we consider the case $\eta = 0$, but we work with the function $u = 1/r$. In this case, the dimensionless correction is given by $\Theta^2/(2b^2)$, where $b = L/E$ is the impact parameter of the light ray.

To derive constraints from light deflection, we consider a photon grazing the solar limb, for which the impact parameter is well approximated by the solar radius: $b \simeq R_\odot = 4.305 \times 10^{43}$ in natural units. We adopt the solar mass $M_\odot = 9.138 \times 10^{37}$.

In General Relativity, the bending angle for such a configuration is $\delta_{\text{GR}} = 4M_\odot/b = 1.7516687''$. Experimental results are commonly parametrized as $\delta_{\text{exp}} = \frac{1}{2}(1 + \gamma) \times 1.7516687''$, where the parameter γ is measured to be 0.99992 ± 0.00012 [51].

The effect of the parameter Θ enters through a multiplicative factor $1 - \Theta^2/(4b^2)$. Matching this factor to the observed value $(1 + \gamma)/2$ results in the bound

$$-9.680 \times 10^{13} \text{ m}^2 \leq \Theta^2 \leq 1.936 \times 10^{13} \text{ m}^2.$$

C. Time delay of light

To compute the Shapiro delay or time delay of light [52], we need also to consider light-like geodesics, but parametrized by the coordinate time t . This can be achieved by working with equation (28) as

$$(\dot{r})^2 = \left(\frac{dr}{dt} \right)^2 = \frac{A^{(\Theta)} D^{(\Theta)} - \frac{\ell^2}{E^2} (A^{(\Theta)})^2}{B^{(\Theta)} D^{(\Theta)}}. \quad (32)$$

We consider that a light ray emitted from the Earth passes close to the surface of the Sun, reaches an obstacle and returns to Earth. The coordinate of minimum distance to the Sun is a turning point characterized by the condition $\dot{r} = 0$. Following Ref. [53], we express the energy and angular momentum in terms of functions of this minimum distance r_{\min} as $L^2/E^2 = D^{(r,\Theta)}(r_{\min})/A^{(r,\Theta)}(r_{\min})$.

For this reason, the time of propagation of the light ray can be written as

$$dt = \pm \frac{1}{A^{(\Theta)}} \frac{1}{\sqrt{\frac{1}{A^{(\Theta)} B^{(\Theta)}} - \frac{D^{(\Theta)}(r_{\min})/A^{(\Theta)}(r_{\min})}{B^{(\Theta)} D^{(\Theta)}}}}. \quad (33)$$

The integration of this expression leads to the approximate expression

$$t = \sqrt{r^2 - r_{\min}^2} + M \left(\sqrt{\frac{r - r_{\min}}{r + r_{\min}}} + 2 \ln \left(\frac{r + \sqrt{r^2 - r_{\min}^2}}{r_{\min}} \right) \right) - \Theta^2 \frac{M}{8r_{\min}r} \sqrt{\frac{r - r_{\min}}{r + r_{\min}}}. \quad (34)$$

When $r \gg r_{\min}$, we find

$$t(r) = r + M + 2M \ln \left(\frac{2r}{r_{\min}} \right) - \Theta^2 \frac{M}{8r_{\min}r}. \quad (35)$$

If $t(r_{E,R})$ is the time taken for a signal to travel from the emitter/Sun to the Sun/receiver. Then after the time taken for the full-round consisting of emission of the ray from the Earth, receiving at a spacecraft, and back to the Earth is

$$T_{\Theta} = 2(r_E + r_R) + 4M \left[1 + \ln \left(\frac{4r_R r_E}{r_{\min}^2} \right) - \frac{\Theta^2}{8r_{\min}} \left(\frac{1}{r_E} + \frac{1}{r_R} \right) \right] = T_{\text{flat}} + \delta T. \quad (36)$$

In the parametrized post-Newtonian formalism, the contribution to this effect is

$$\delta T = 4M \left(1 + \frac{1+\gamma}{2} \ln \left(\frac{4r_R r_E}{r_{\min}^2} \right) \right). \quad (37)$$

Data from the Cassini mission [54, 55] constrain the parameter γ as $|\gamma - 1| < 2.3 \times 10^{-5}$. Let us assume the distance r_E as the one between the Earth and the Sun, i.e., as one astronomical unit $r_E = 1 \text{ AU}$. Also, when the measurement that set this bound on γ was performed, the Cassini probe was located at $r_R = 8.46 \text{ AU}$ from the Sun, and the minimal radial distance was $r_{\min} = 1.6 R_{\odot}$, where R_{\odot} is the solar radius. Endowed with these tools and using the uncertainty in the determination of γ , we are led to the following constrain on the non-commutative parameter

$$|\Theta^2| \leq 1.565 \times 10^{18} \text{ m}^2. \quad (38)$$

A presentation of the resulting parameter bounds is given in Table I.

VI. CONCLUSION

In this work, the quantum properties of a Schwarzschild-like black hole constructed within non-commutative gauge gravity were investigated by adopting the Moyal twist $\partial_t \wedge \partial_{\theta}$, which ensured a well-defined surface gravity and, consequently, a consistent thermodynamic description. The

Table I: Bounds for Θ^2 derived from Solar System tests.

Solar System Test	Constraints (m^2)
Mercury precession	$-3.725 \times 10^9 \leq \Theta^2 \leq 1.862 \times 10^{10}$
Light deflection	$-9.680 \times 10^{13} \leq \Theta^2 \leq 1.936 \times 10^{13}$
Shapiro time delay	$-1.565 \times 10^{18} \leq \Theta^2 \leq 1.565 \times 10^{18}$

corrected construction of non-commutative black hole geometries was taken as the starting point based on [23], and the resulting spacetime was shown to preserve the classical horizon location and surface gravity.

Quantum particle creation was analyzed using the tunneling formalism for both bosonic and fermionic fields. For bosons, the tunneling probability and the corresponding occupation number were derived by incorporating backreaction effects, leading to emission spectra that deviated from the purely thermal Schwarzschild case. For fermions, the curved-spacetime Dirac equation was solved within a semiclassical approximation, and the resulting particle production rate exhibited a suppression as the non-commutative parameter increased. These results demonstrated that, although the Hawking temperature itself remained unchanged, the non-commutative deformation modified the detailed structure of the emission process.

The evaporation dynamics were subsequently examined through an effective *Stefan–Boltzmann* approach combined with the high-energy absorption cross section. It was found that the non-commutative corrections enhanced the radiative emission rate and reduced the total evaporation time, in agreement with the qualitative behavior observed in other non-commutative black hole scenarios. The absence of a stable remnant in the present model implied that the evaporation proceeded until complete mass loss.

Finally, bounds on the non-commutative parameter Θ were inferred from classical solar system tests, namely the perihelion precession of Mercury, light deflection, and Shapiro time delay. The resulting constraints restricted the allowed magnitude of Θ^2 and justified the perturbative regime adopted in the analysis.

Acknowledgments

A.A.A.F. is supported by Conselho Nacional de Desenvolvimento Científico e Tecnológico (CNPq) and Fundação de Apoio à Pesquisa do Estado da Paraíba (FAPESQ), project numbers 150223/2025-0 and 1951/2025. I. P. L. was partially supported by the National Council for Scientific and Technological Development - CNPq, grant 312547/2023-4. I. P. L. would like to acknowledge networking support by the COST Action BridgeQG (CA23130), the COST Action RQI

(CA23115) and the COST Action FuSe (CA24101) supported by COST (European Cooperation in Science and Technology).

Data Availability Statement

Data Availability Statement: No Data associated with the manuscript

- [1] R. J. Szabo, “Quantum field theory on noncommutative spaces,” *Physics Reports*, vol. 378, no. 4, pp. 207–299, 2003.
- [2] N. Seiberg and E. Witten, “String theory and noncommutative geometry,” *Journal of High Energy Physics*, vol. 1999, no. 09, p. 032, 1999.
- [3] R. J. Szabo, “Symmetry, gravity and noncommutativity,” *Classical and Quantum Gravity*, vol. 23, no. 22, p. R199, 2006.
- [4] A. F. Ferrari, H. O. Girotti, M. Gomes, A. Y. Petrov, A. Ribeiro, and A. J. Da Silva, “On the finiteness of noncommutative supersymmetric qed3 in the covariant superfield formulation,” *Physics Letters B*, vol. 577, no. 1-2, pp. 83–92, 2003.
- [5] A. H. Chamseddine, “Deforming einstein’s gravity,” *Physics Letters B*, vol. 504, no. 1-2, pp. 33–37, 2001.
- [6] R. B. Mann and P. Nicolini, “Cosmological production of noncommutative black holes,” *Physical Review D*, vol. 84, no. 6, p. 064014, 2011.
- [7] M. Karimabadi, S. A. Alavi, and D. M. Yekta, “Non-commutative effects on gravitational measurements,” *Classical and Quantum Gravity*, vol. 37, no. 8, p. 085009, 2020.
- [8] Y. Zhao, Y. Cai, S. Das, G. Lambiase, E. Saridakis, and E. Vagenas, “Quasinormal modes in non-commutative schwarzschild black holes,” *Nuclear Physics B*, vol. 1004, p. 116545, 2024.
- [9] L. Modesto and P. Nicolini, “Charged rotating noncommutative black holes,” *Physical Review D*, vol. 82, no. 10, p. 104035, 2010.
- [10] A. A. Araújo Filho, J. R. Nascimento, A. Y. Petrov, P. J. Porfírio, and A. Övgün, “Effects of non-commutative geometry on black hole properties,” *Physics of the Dark Universe*, vol. 46, p. 101630, 2024.
- [11] M. A. Anacleto, F. A. Brito, J. A. V. Campos, and E. Passos, “Absorption and scattering of a noncommutative black hole,” *Phys. Lett. B*, vol. 803, p. 135334, 2020.
- [12] N. Heidari, H. Hassanabadi, A. A. Araújo Filho, and J. Kriz, “Exploring non-commutativity as a perturbation in the schwarzschild black hole: quasinormal modes, scattering, and shadows,” *The European Physical Journal C*, vol. 84, no. 6, p. 566, 2024.

- [13] A. A. Araújo Filho, J. R. Nascimento, A. Y. Petrov, P. J. Porfírio, and A. Övgün, “Properties of an axisymmetric lorentzian non-commutative black hole,” *Physics of the Dark Universe*, vol. 47, p. 101796, 2025.
- [14] J. Lopez-Dominguez, O. Obregon, M. Sabido, and C. Ramirez, “Towards noncommutative quantum black holes,” *Physical Review D*, vol. 74, no. 8, p. 084024, 2006.
- [15] J. A. V. Campos, M. Anacleto, F. A. Brito, and E. Passos, “Quasinormal modes and shadow of noncommutative black hole,” *Scientific Reports*, vol. 12, no. 1, p. 8516, 2022.
- [16] Y. S. Myung, Y.-W. Kim, and Y.-J. Park, “Thermodynamics and evaporation of the noncommutative black hole,” *Journal of High Energy Physics*, vol. 2007, no. 02, p. 012, 2007.
- [17] A. A. Araújo Filho, “Particle production induced by a Lorentzian non-commutative spacetime,” *Annals Phys.*, vol. 481, p. 170167, 2025.
- [18] M. Sharif and W. Javed, “Thermodynamics of a bardeen black hole in noncommutative space,” *Canadian Journal of Physics*, vol. 89, no. 10, pp. 1027–1033, 2011.
- [19] K. Nozari and B. Fazlpour, “Thermodynamics of noncommutative schwarzschild black hole,” *Modern Physics Letters A*, vol. 22, no. 38, pp. 2917–2930, 2007.
- [20] R. Banerjee, B. R. Majhi, and S. Samanta, “Noncommutative black hole thermodynamics,” *Physical Review D*, vol. 77, no. 12, p. 124035, 2008.
- [21] K. Nozari and B. Fazlpour, “Reissner-nordstr\{o\} m black hole thermodynamics in noncommutative spaces,” *arXiv preprint gr-qc/0608077*, 2006.
- [22] M. Chaichian, A. Tureanu, and G. Zet, “Corrections to Schwarzschild solution in noncommutative gauge theory of gravity,” *Phys. Lett. B*, vol. 660, pp. 573–578, 2008.
- [23] T. Jurić, A. N. Kumara, and F. Požar, “Constructing noncommutative black holes,” *Nucl. Phys. B*, vol. 1017, p. 116950, 2025.
- [24] A. Touati and Z. Slimane, “Quantum tunneling from Schwarzschild black hole in non-commutative gauge theory of gravity,” *Phys. Lett. B*, vol. 848, p. 138335, 2024.
- [25] A. Touati and S. Zaim, “Thermodynamic properties of Schwarzschild black hole in non-commutative gauge theory of gravity,” *Annals Phys.*, vol. 455, p. 169394, 2023.
- [26] A. A. A. Filho, S. Zare, P. J. Porfírio, J. Kriz, and H. Hassanabadi, “Thermodynamics and evaporation of a modified Schwarzschild black hole in a non-commutative gauge theory,” *Phys. Lett. B*, vol. 838, p. 137744, 2023.
- [27] N. Heidari, H. Hassanabadi, A. A. A. Filho, J. Kriz, S. Zare, and P. J. Porfírio, “Gravitational signatures of a non-commutative stable black hole,” *Phys. Dark Univ.*, vol. 43, p. 101382, 2024.
- [28] A. A. Araújo Filho and I. P. Lobo, “Comment on “Quantum tunneling from Schwarzschild black hole in non-commutative gauge theory of gravity”,” *Phys. Lett. B*, vol. 868, p. 139771, 2025.

[29] A. A. Araújo Filho and I. P. Lobo, “Comment on “Thermodynamic properties of Schwarzschild black hole in non-commutative gauge theory of gravity”,” *Annals Phys.*, vol. 485, p. 170323, 2026.

[30] N. Heidari, A. A. Araújo Filho, and I. P. Lobo, “Non-commutativity in Hayward spacetime,” *JCAP*, vol. 09, p. 051, 2025.

[31] M. K. Parikh and F. Wilczek, “Hawking radiation as tunneling,” *Physical review letters*, vol. 85, no. 24, p. 5042, 2000.

[32] L. Vanzo, G. Acquaviva, and R. Di Criscienzo, “Tunnelling methods and Hawking’s radiation: achievements and prospects,” *Classical and Quantum Gravity*, vol. 28, no. 18, p. 183001, 2011.

[33] M. K. Parikh, “Energy conservation and Hawking radiation,” *arXiv preprint hep-th/0402166*, 2004.

[34] X. Calmet, S. D. H. Hsu, and M. Sebastianutti, “Quantum gravitational corrections to particle creation by black holes,” *Phys. Lett. B*, vol. 841, p. 137820, 2023.

[35] R. Kerner and R. B. Mann, “Fermions tunnelling from black holes,” *Classical and Quantum Gravity*, vol. 25, no. 9, p. 095014, 2008.

[36] Y. C. Ong, “An effective black hole remnant via infinite evaporation time due to generalized uncertainty principle,” *Journal of High Energy Physics*, vol. 2018, no. 10, pp. 1–11, 2018.

[37] A. A. Araújo Filho, “Particle production induced by a lorentzian non-commutative spacetime,” *Annals of Physics*, p. 170167, 2025.

[38] W. A. Hiscock and L. D. Weems, “Evolution of charged evaporating black holes,” *Physical Review D*, vol. 41, no. 4, p. 1142, 1990.

[39] D. N. Page, “Particle emission rates from a black hole. ii. massless particles from a rotating hole,” *Physical Review D*, vol. 14, no. 12, p. 3260, 1976.

[40] X. Liang, Y.-S. An, C.-H. Wu, and Y.-P. Hu, “Einstein-horndeski gravity and the ultra slowly evaporating black hole,” *Physics Letters B*, p. 139303, 2025.

[41] S. W. Hawking, “Particle creation by black holes,” in *Euclidean quantum gravity*, pp. 167–188, World Scientific, 1975.

[42] N. Heidari and A. A. Araújo Filho, “Quantum particle production and radiative properties of a new bumblebee black hole,” 12 2025.

[43] A. A. Araújo Filho, N. Heidari, and I. P. Lobo, “A non-commutative Kalb-Ramond black hole,” *JCAP*, vol. 09, p. 076, 2025.

[44] Y. Décanini, G. Esposito-Farese, and A. Folacci, “Universality of high-energy absorption cross sections for black holes,” *Physical Review D*, vol. 83, no. 4, p. 044032, 2011.

[45] U. Papnoi and F. Atamurotov, “Rotating charged black hole in 4d einstein–gauss–bonnet gravity: Photon motion and its shadow,” *Physics of the Dark Universe*, vol. 35, p. 100916, 2022.

[46] A. Addazi *et al.*, “Quantum gravity phenomenology at the dawn of the multi-messenger era—A

review,” *Prog. Part. Nucl. Phys.*, vol. 125, p. 103948, 2022.

- [47] R. Alves Batista *et al.*, “White paper and roadmap for quantum gravity phenomenology in the multi-messenger era,” *Class. Quant. Grav.*, vol. 42, no. 3, p. 032001, 2025.
- [48] H. Goldstein, C. Poole, and J. Safko, *Classical Mechanics*. San Francisco, USA: Addison-Wesley, 3rd ed., 2002.
- [49] R. Casana, A. Cavalcante, F. P. Poulis, and E. B. Santos, “Exact Schwarzschild-like solution in a bumblebee gravity model,” *Phys. Rev. D*, vol. 97, no. 10, p. 104001, 2018.
- [50] K. Yang, Y.-Z. Chen, Z.-Q. Duan, and J.-Y. Zhao, “Static and spherically symmetric black holes in gravity with a background Kalb-Ramond field,” *Phys. Rev. D*, vol. 108, no. 12, p. 124004, 2023.
- [51] S. Lambert and C. Le Poncin-Lafitte, “Improved determination of γ by vlbi,” *Astronomy & Astrophysics*, vol. 529, p. A70, 2011.
- [52] I. I. Shapiro, “Fourth Test of General Relativity,” *Phys. Rev. Lett.*, vol. 13, pp. 789–791, 1964.
- [53] R.-B. Wang, S.-J. Ma, J.-B. Deng, and X.-R. Hu, “Estimating the strength of Lorentzian distribution in non-commutative geometry by solar system tests,” 11 2024.
- [54] B. Bertotti, L. Iess, and P. Tortora, “A test of general relativity using radio links with the Cassini spacecraft,” *Nature*, vol. 425, pp. 374–376, 2003.
- [55] C. M. Will, “The Confrontation between General Relativity and Experiment,” *Living Rev. Rel.*, vol. 17, p. 4, 2014.